

Energy Dissipation in Multichromophoric Single Dendrimers

F. C. DE SCHRYVER,^{*,†} T. VOSCH,[†] M. COTLET,[†] M. VAN DER AUWERAER,[†] K. MÜLLEN,[‡] AND J. HOFKENS^{*,†}

Department of Chemistry, KULeuven, Celestijnenlaan 200F, B-3001 Heverlee, Belgium, and Max-Planck-Institute für Polymerforschung, Ackermannweg 10, 55128 Mainz, Germany

Received July 13, 2004

ABSTRACT

Single-molecule spectroscopy of well-chosen dendritic multichromophoric systems allows investigation of fundamental photophysical processes such as energy or electron transfer in much greater detail than the respective ensemble measurements. In dendrimers with multiple chromophores, energy hopping and transfer to the chromophore with the energetically lowest S_1 state was observed. If more than one chromophore is in an excited state in one molecule, annihilation, either singlet–triplet or singlet–singlet, can occur. In the latter case, a higher singlet state is populated opening new deactivation pathways. In the presence of an electron donor, reversible electron transfer could be observed, and the rate constants of forward and backward electron transfer were established. The value of these rate constants fluctuates time-correlated with the rotational motion of the dendrimer arms and the mobility of the embedding matrix.

Introduction

The excited-state properties of multichromophoric systems¹ have been of interest to our research group, initially from the more photochemical point of view, as possible intermediates in stepwise photopolymerization¹ and intramolecular excited-state interactions such as excimer and exciplex formation.² At present, the fundamental

F. C. De Schryver was born in 1939 and got his Ph.D. in 1964 at the KULeuven. He has been professor at the KULeuven since 1969. He is recipient of a Humboldt and a Max Planck Research Award. His interests are in time- and space-resolved chemistry.

T. Vosch was born in 1976 and studied and got his Ph.D. in 2003 at the KULeuven where he is presently a postdoctoral fellow working in the area of single-molecule spectroscopy.

M. Cotlet was born in 1969 in Roumania and studied at the KULeuven where he got his Ph.D. in 2002. He is presently a Director-sponsored postdoctoral fellow at Los Alamos working in the area of single-molecule spectroscopy.

M. Van der Auweraer was born in 1955 and got his Ph.D. at the KULeuven in 1981 where he became a professor in 1989 having been a postdoctoral fellow of the Flemish Science Foundation. His interests are in ultrafast spectroscopy.

K. Müllen was born in 1947, got his Ph.D. at the University of Basel, Switzerland, in 1972 and joined the Max-Planck-Society in 1989 as one of the directors of the Max-Planck Institute for Polymer Research. His interests are in synthesis and physical chemistry of large conjugated π systems and rigid dendrimers.

J. Hofkens was born in 1966 and got his Ph.D. at the KULeuven in 1993. He has been since 2001 professor at the KULeuven and the Université Catholique de Louvain. He is interested in single-molecule spectroscopy and fluorescence microscopy.

understanding of energy dissipation pathways in multichromophoric systems is of interest in material science and in photobiology, for example, in conjugated polymers³ and in light-harvesting systems or in autofluorescent proteins.⁴ The complexity of some of these systems has driven us not only to investigate the time dependence but also to attempt to spatially resolve the photoinduced process.

The development of rigid dendritic structures⁵ opened the possibility to initiate a project that allows fundamental excited-state processes to be studied at the single-molecule level in multichromophoric systems in which the relative position and orientation of the chromophores would be fixed in space and determined by the synthetic route. In view of the requirements of single-molecule spectroscopy, rylene dyes, having large molar extinction coefficients in the visible region of the spectrum, a high quantum yield of fluorescence, and excellent photostability, were chosen as chromophores.⁶ In parallel and absolutely essential to the full understanding of the single-molecule behavior, a detailed ensemble time-resolved spectroscopy study from femto- to microsecond time scale was performed, but these data will only be mentioned where necessary, and the added value of the single-molecule approach will be stressed.

The fundamental photophysical processes investigated here are categorized as processes based on electronic energy transfer and processes based on photoinduced electron transfer. For the former process, if the multichromophoric system has only weak interchromophoric interactions in the ground state, one can describe the energy-transfer processes within the framework of the Förster model (FRET).⁷ For identical chromophores, energy hopping can occur, while, if different, structurally, energetically, or both, directional energy transfer is possible. In addition, under conditions of multiple excitations in one molecule, annihilation processes can occur.

Photoinduced electron transfer will be possible if the driving force, which is the change in free enthalpy, is adequate.

These processes were investigated in dendritic structures for which the core is either a sp^3 carbon (Figure 1a) or a rigid dye (Figure 8b) and is decorated with polyphenylene rigid dendritic arms (Figure 1b), which are substituted by one or more chromophores.

Excitation Energy Transfer

Between Structurally Identical Chromophores. The processes important in multichromophoric systems with structurally identical chromophores will be highlighted based on dendrimers having a central sp^3 carbon (C) and decorated with a variable number of perylenemonoimide

* To whom correspondence should be addressed. Fax: +3216327989. E-mail addresses: Frans.Deschryver@chem.kuleuven.ac.be; Johan.Hofkens@chem.kuleuven.ac.be.

[†] KULeuven.

[‡] Max-Planck-Institut für Polymerforschung.

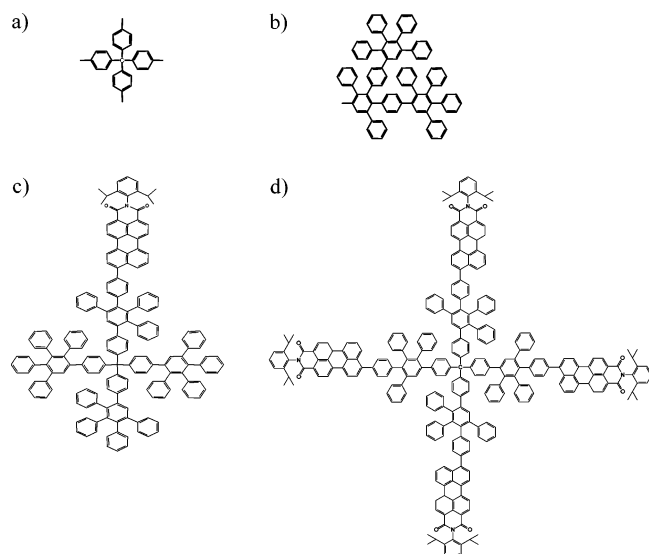


FIGURE 1. Core of a dendrimer (a), polyphenylene arm (b), and chemical structure of C1P1p (c) and C1P4p (d).

(P) chromophores in the para position of a phenyl group at the rim of the rigid polyphenylene arms (Figure 1). In Figure 1c,d, the structures of the first generation dendrimer with one P, C1P1p, used as a model system and with four P's, C1P4p, are given. Geometry optimization of C1P4p shows that the center to center distance between the chromophores is approximately 3 nm.

The absorption and emission spectra of C1P1p and C1P4p in toluene at room temperature are superimposable (Figure 2a). The fluorescence quantum yield of C1P1p and of C1P4p equals 0.98 ± 0.05 , while their fluorescence decay time is monoexponential and equals 4 ns. This clearly shows the absence of strong coupling and the applicability of the Förster model. Time-resolved fluorescence depolarization experiments of C1P4p show biexponential anisotropy fluorescence decay with values of 1.72 and 0.05 ns. While the 1.72 ns decay can be associated with a rotational correlation decay time of the whole dendrimer, the fast depolarization decay time of 0.05 ns can be related to FRET among identical P's.

From these data, a rate constant of $5 \times 10^9 \text{ s}^{-1}$ for FRET between identical P's could be extracted.⁸ If C1P4p is excited under high photon flux, two excited states (S_1) can be present at the same time in a single molecule. If the S_1-S_0 transition of one chromophore is in resonance with a S_1-S_n transition of the other chromophore, energy transfer between the excited singlet states can occur resulting in one excited state (singlet–singlet annihilation). The rate constant of this process, observed at the ensemble level,⁹ equals $2 \times 10^{11} \text{ s}^{-1}$. Both FRET processes observed at the ensemble level⁷ can in view of equal structural aspects (distance and orientation of the chromophores in the dendrimer) be visualized by the spectral overlap of the states involved in the process (Figure 2a,b). Similarly one could consider, based on overlap between the triplet absorption and fluorescence, the possibility of singlet–triplet annihilation, a process not observed at the ensemble level (Figure 2c).

Analysis of a single-molecule fluorescence intensity trajectory of C1P1p (Figure 3a) in a 100 nm thick spin-coated film of poly(methyl methacrylate) (PMMA) allowed the determination of the triplet lifetime of P, which equals 1 ms, and its intersystem crossing rate constant of $6 \times 10^3 \text{ s}^{-1}$.¹⁰ Figure 3b shows a fluorescence trajectory of a C1P4 molecule embedded in a PMMA film under nitrogen atmosphere using 488 nm excitation with four stable fluorescence intensity levels. This indicates that when one chromophore is bleached, it does not act as a quencher. The triplet related off events of C1P4p (Figure 3b) show the collective behavior of the chromophores. If one chromophore goes to the triplet state, this also quenches the fluorescence of the other chromophore as can be seen in Figure 3b. A similar behavior was also observed in other P-containing systems^{10–12}. This is an example of **singlet–triplet annihilation** (Figure 2c).

Within the long lifetime of the triplet state, a second chromophore can be excited, and in C1P4p, a S_1 and a T_1 state are present. If the triplet state exhibits transitions into higher excited triplet states, T_n , that are in resonance with the $S_1 \rightarrow S_0$ transition, energy transfer from the excited singlet state to the triplet state can occur. Because T_1 to T_n is an allowed transition, the process is FRET-based. The Förster radius, R_0 , of 7.86 nm and the interchromophoric distance of 3 nm on average lead to an efficiency of approximately 100% (Figure 2d). This also suggests that the other less frequent occurrences of longer off times might be related to overlap of the fluorescence spectrum with other transient species, such as an ion radical or radical formed from P and having an absorption in the visible.¹⁰

By detection of this annihilation process, not observed at the ensemble level, single-molecule spectroscopy deepens the insight in the above-mentioned excited-state processes. Quantum-chemical calculations of the various energy-transfer processes support the higher efficiency of the annihilation processes with respect to singlet hopping.^{12b}

Using polarized fluorescence intensity trajectories, one can visualize the energy hopping process at the single-molecule level. The parallel and perpendicular components of the stepwise changes in fluorescence intensity in the transient as shown in Figure 4, explained by consecutive bleaching of the chromophores, were recorded with two detectors (polarized transients). Figure 4 shows four distinct levels in the polarization trajectory, p , of a C1P4p molecule embedded in Zeonex indicating that the excitation hops between different P's. The polarization transient and corresponding histogram (Figure 4) of this spatially well-defined system indicate that emission occurs at all times from the chromophore that is lowest in energy.¹³

This implies one chromophore acting as a fluorescent trap while the other chromophores are communicating via excitation energy hopping and directional energy transfer to the energetically lowest P, based on the overlap between the ensemble absorption and emission spectra and the calculated Förster radius of 4.78 nm (Figure 2a,d).

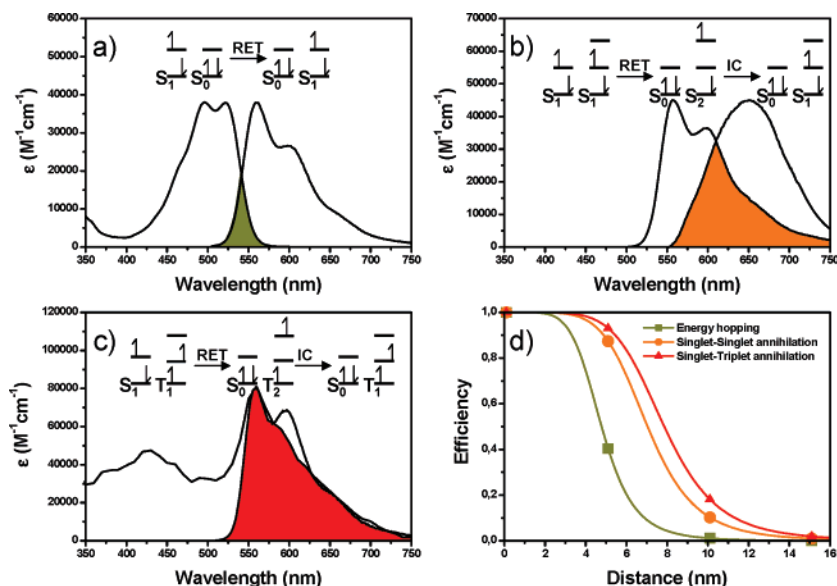


FIGURE 2. Panel a shows the superimposed absorption and emission spectra of C1P1p and C1P4p in toluene (spectral overlap indicated in color). The inset shows the scheme for energy hopping. Panel b shows transient absorption (S_1 – S_n) and emission spectra of C1P1p in toluene (spectral overlap indicated in color). The inset shows the scheme for singlet–singlet annihilation. Panel c shows triplet absorption and emission spectra of C1P1p in toluene (spectral overlap indicated in color). The inset shows the scheme for singlet–triplet annihilation. Panel d shows efficiency as a function of distance between two chromophores for the three FRET processes possible in C1P4p.

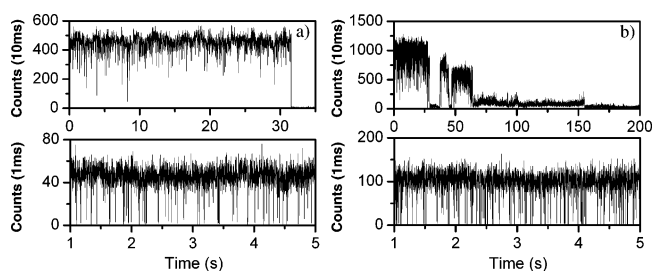


FIGURE 3. Panel a shows (top) the fluorescence intensity trajectory of a C1P1p molecule embedded in PMMA using circular polarized CW light and (bottom) zoom of first 5 s of the trace to illustrate the on/off blinking. Panel b shows (top) the fluorescence intensity trajectory of a C1P4p molecule in PMMA and (bottom) zoom of the first 5 s of the transient depicted in the top panel, showing the triplet blinking.

That each chromophore in turn can eventually act as energy sink could be further demonstrated in C1P4p by measuring the orientation of the fluorescent trap in the multichromophoric entity using a wide-field defocusing technique that allows direct probing of the emission dipole orientation.¹⁴ C1P4p molecules were embedded in a 25 nm Zeonex film. The patterns shown in Figure 5 were observed during the indicated consecutive period, while each image was obtained by integrating the signal during an exposure time of 10 s.

The emission pattern of a single C1P4p molecule changes as function of time. The patterns provide direct evidence that different chromophores of the C1P4p emit in time as different dipole orientations are observed successively. By comparison of the recorded experimental patterns with simulated patterns,¹⁴ we attribute, following the sequence shown in Figure 5, the first pattern as due to a chromophore with an emission dipole oriented in-plane along the x -axis. The second pattern is due to

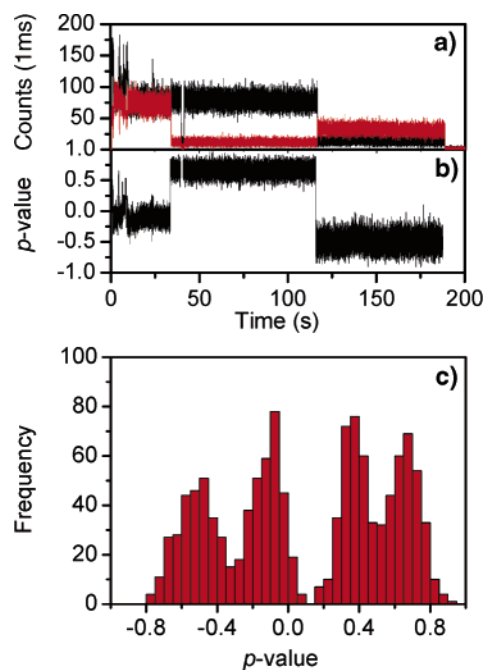


FIGURE 4. Example of (a) a transient of C1P4p where the parallel and perpendicular component were detected separately, (b) the polarization value of the trace in panel a, and (c) a histogram of the four p levels of the trace in panel b.

another in-plane emission dipole with an angle of -45° with respect to the x -axis. The third and fourth patterns correspond to an out-of-plane emission dipole and to an in-plane emission dipole with an angle of $+45^\circ$ with respect to the x -axis, respectively.¹⁵

The observation of **singlet–singlet annihilation** as a fast, excitation-intensity-dependent decay component in time-resolved fluorescence measurements is impossible in single-molecule spectroscopy due to the limited time



FIGURE 5. Emission patterns taken from a series of consecutive defocused images recorded for a single C1P4p in a 100 nm Zeonex film. Images were recorded at $1\ \mu\text{m}$ defocusing to the glass surface. Time intervals, during which successive patterns have been observed, are listed underneath the images. The emission pattern of a single C1P4p molecule changes as function of time. The patterns provide direct evidence that different chromophores of the C1P4p emit in time as different dipole orientations.

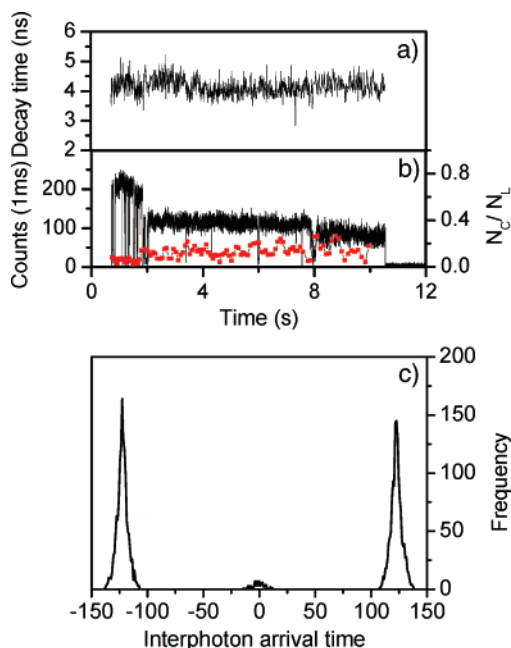


FIGURE 6. A typical time trace of (a) fluorescence intensity, (b) fluorescence decay time and (c) the ratio of the central peak to the average of the lateral peaks (N_c/N_l) measured from C1P4p embedded in zeonex and (c) the interphoton arrival time distribution obtained from the first fluorescence intensity level of the time trace.

resolution (~ 300 ps) presently provided by avalanche photodiodes used for detection. Indirect evidence for the process can however be obtained. A saturation of the fluorescence intensity with increasing excitation power impinging on an individual multichromophoric system eventually points toward an annihilation process. Unambiguous evidence for the annihilation phenomenon can be obtained because for a single chromophore the probability of emitting two consecutive photons drops to zero for time intervals shorter than the excited-state lifetime. This property of the photon arrival time statistics, termed photon antibunching, has been measured at room temperature under pulsed laser illumination for individual molecules by measuring and histogramming the interphoton arrival times.¹⁶ Hence, for a single emitter, the zero peak, which represents pairs of fluorescence photons generated during the same laser pulse, is necessarily vacant as long as the laser pulse width is much smaller than the fluorescence lifetime of the molecule. Thus, for C1P4p under pulsed excitation conditions, the absence

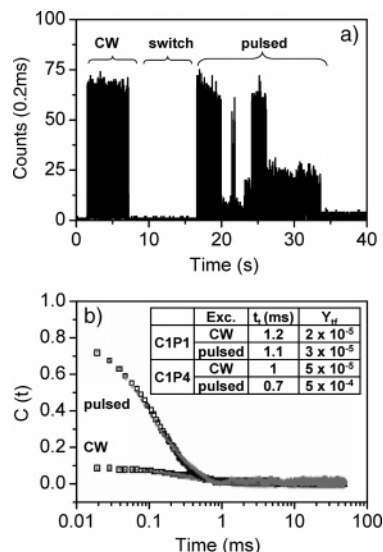
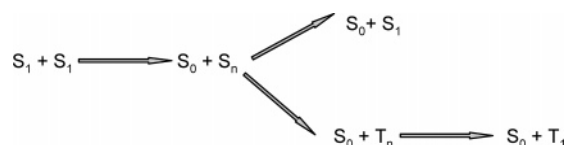


FIGURE 7. Panel a shows the fluorescence intensity time trace of an individual C1P4p molecule measured by CW excitation and pulsed excitation embedded in PMMA under N_2 flow. From 7 to 16 s, the excitation source was switched from CW to pulsed excitation. Panel b shows autocorrelation curves built from the CW excitation period and the first intensity level of the pulsed excitation period in the time trace in panel a. The inset shows the average triplet lifetime (τ_t) and triplet formation yield (Y_{tf}) of C1P1p and C1P4p calculated from the CW excitation period and from the first intensity level of the pulsed excitation period.

Scheme 1. Photophysical Processes That Can Occur When in One Molecule Two Excited Chromophores Are Present



of the peak at zero in the interphoton arrival time distribution would indicate the existence of an efficient singlet–singlet annihilation process.¹⁷

Figure 6 shows an example of a C1P4p molecule in Zeonex. The absence of the central peak shows that C1P4p acts as a single emitter. A similar observation was made for other multichromophoric dendrimers.^{10,18,19} Detailed analysis of the fluorescence trajectories reveals an additional triplet formation pathway the efficiency of which depends on the chromophore number and excitation conditions (continuous wave (CW) or pulsed) indicating that efficient singlet–singlet annihilation and subsequent intersystem crossing from higher excited states, S_n , are the underlying photophysical mechanism as illustrated by Figure 7 and Scheme 1.

In Figure 7a, C1P4p was first excited by a CW laser for several seconds; then excitation was switched to pulsed excitation at the same wavelength and average excitation power until photobleaching occurred. The autocorrelation curves show that triplet formation is more frequent upon pulsed excitation compared to CW. The average τ_t and Y_{tf} of C1P1p and C1P4p obtained by CW and pulsed excitation are depicted in the inset of Figure 7b. For C1P4p, the value of Y_{tf} calculated from the first intensity level in the

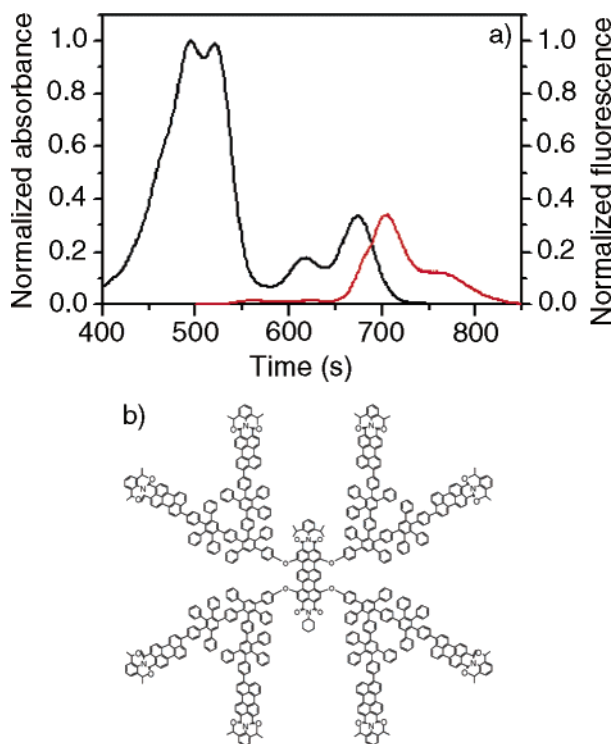


FIGURE 8. Structure (b) of T2P8 and ensemble steady-state absorption and emission spectra (a) in toluene in the 400–800 nm range.

trace is 10 times higher than that calculated from the CW excitation, and the τ_t in the pulsed excitation period is slightly shorter than that in the CW excitation and is also shorter than that of C1P1p.¹⁸ On the other hand, for C1P1p, no influence of the excitation condition is observed. These results indicate that for C1P4p the triplet parameters are influenced only under pulsed excitation conditions. While multiple chromophores can be excited at the same time using pulsed excitation, under CW excitation this probability is very low. Therefore multiple chromophore excitation plays an important role in opening this additional photophysical pathway. The increase of Y_{tr} in C1P4p can be explained by the processes described in Scheme 1.

S_1 – S_1 annihilation leading to a S_n state followed by internal conversion to S_1 , which is the most important pathway, competes with intersystem crossing from S_n to T_n , and this process leads to an increase of the observed triplet formation yield. This process, only revealed at the single-molecule level, exemplifies the capability of single-molecule spectroscopy to uncover information complementary to the ensemble data and to investigate higher excited-state processes.

Between Structurally Different Chromophores. The structure of the investigated molecular system and the corresponding steady-state absorption and emission spectra in toluene are depicted in Figure 8. The dendrimer T2P8 consists of a terrylenediimide (T) core and eight P's at the rim of the polyphenylene branches (2 indicates second generation). T2P8 was previously investigated at the ensemble level by means of stationary and time-resolved fluorescence spectroscopy,²⁰ and the data sug-

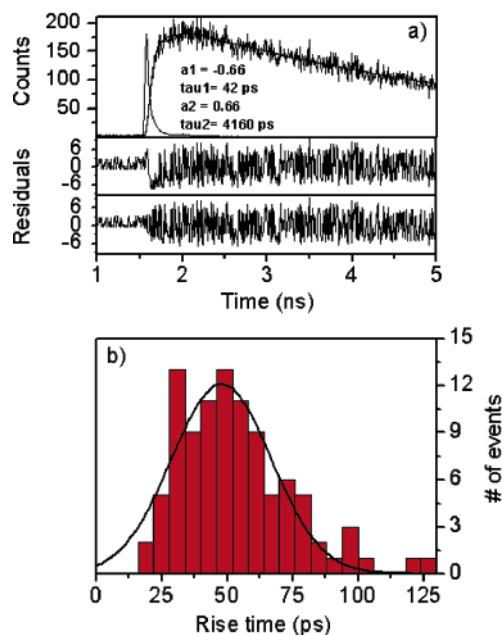


FIGURE 9. Panel a shows (top) fluorescence decay histogram (gray line) recorded with an MCP-PMT detector and accounting for the acceptor emission of a single T2P8 molecule in Zeonex upon selective 488-nm excitation of the donors. The instrumental response function of the system (black dotted line) and the biexponential fit curve (black full line) are also shown. The middle and bottom panels show residual graphs for mono- (gray line) and biexponential (black line) fits. The residual graphs show that a monoexponential fit gives erroneous results in the rise, whereas a biexponential fit (solid line in the decay) with a negative preexponential factor for the short time constant gives a good result. Panel b shows a histogram of the rise times accounting for 100 single T2P8.

gested the presence of two kinetically different energy-transfer processes. The use of avalanche photodiodes (APDs) with their limited time resolution makes the detection of fast kinetic components of directional FRET from P to T, as suggested by the ensemble solution time-resolved data, impossible.²⁰ The exceptional photostability of T allows the use of a multichannel plate detector (~ 23 ps response time), which is more suited to detect a fast rise term if one uses appropriate deconvolution procedures. For each single molecule, all the detected photons from the acceptor were used to build a decay histogram in 1024 channels with a channel width of 3.4 ps. The recorded fluorescence decays were analyzed by using reference convolution (erythrosine in aqueous solution, 85 ps decay time) with a biexponential model function with positively and negatively contributing time constants and maximum likelihood estimator (MLE) fitting. In all cases, the ratio of the preexponential factors accounting for the contributions of the recovered time constants was around -1.0 ± 0.2 . This demonstrates that the excited state of T in T2P8 is built up only from FRET from P. A typical analyzed single-molecule decay accounting for an individual T2P8 molecule is given in Figure 9a. The histogram accounting for the rise components detected from T2P8 does not show a bimodal distribution as one would expect on the basis of ensemble solution time-

resolved data.²⁰ Instead, a broad distribution with a mean value of 48 ps is observed (Figure 9b).

This finding points to a broad range of FRET processes at the single-molecule level, rather than two classes of structural isomers as assumed on the basis of the ensemble time-resolved data. A broad range of FRET processes implies here a broad range of interchromophoric distances and orientations between the donor and acceptor chromophores in the dendrimers when immobilized in Zeonex.²¹

Electron Transfer

Electron transfer (ET) involves a pair of electron-donor and -acceptor entities, and its efficiency scales exponentially with the donor–acceptor distance. However, whereas a highly efficient FRET results in fluorescence emitted mainly from the acceptor chromophore, a highly efficient ET usually leads to a strong quenching of the fluorescence of the emitting chromophore. Thus, reports on single-molecule photoinduced ET are rather limited in number,²² in contrast to reports on single-molecule FRET. A particular situation of ET refers to the case when the locally excited state (LES) and the charge-separated state (CSS) are close in energy. In this case, upon excitation, the LES deactivates mainly via forward ET to the CSS and, if the radiationless deactivation of the CSS to the ground state (GS) is inefficient (*vide infra*), the CSS decays via the LES by reverse ET. As a net result, the emitted fluorescence is delayed but can retain a high quantum yield.²³ The structure of the electron donor–acceptor system is depicted in Figure 10.²⁴

Femtosecond transient spectroscopy of PDN16 in toluene shows formation of a radical anion of PD (data not shown), while the fluorescence quantum yield equals 0.65 for PDN16 (1 for PDN0), and the fluorescence decays multiexponentially with decay times spanning a broad range from tens of picoseconds to tens of nanoseconds, substantially longer than the 6 ns of the monoexponentially decaying PDN0. Ensemble data show that reversible ET is present, that is, forward ET from LES to CSS and reverse ET from CSS to LES (Scheme 2).

In polystyrene (PS), single PDN16 fluoresces at an average photon count rate of 20–200 counts/10 ms if blanketed with a nitrogen stream. Single molecules emitting at low photon count rate show multiexponential fluorescence decay with time components as long as 15 ns. The photon count rate vs the average decay time correlations for PS spread to longer decay times/lower photon count rates, a signature of the reversible ET. Assuming that single-molecule decay components longer than 10 ns relate to delayed fluorescence and hence to reverse ET, within the probed population reversible ET is detected in 10% of PDN16.

Shown in Figure 11c is the lifetime trajectory of a single PDN16 molecule in Zeonex (ZE), a mimic of methylcyclohexane in which PDN16 does not undergo electron transfer, using bins of 500 photons for which lifetimes were estimated by MLE fitting with a single-exponential

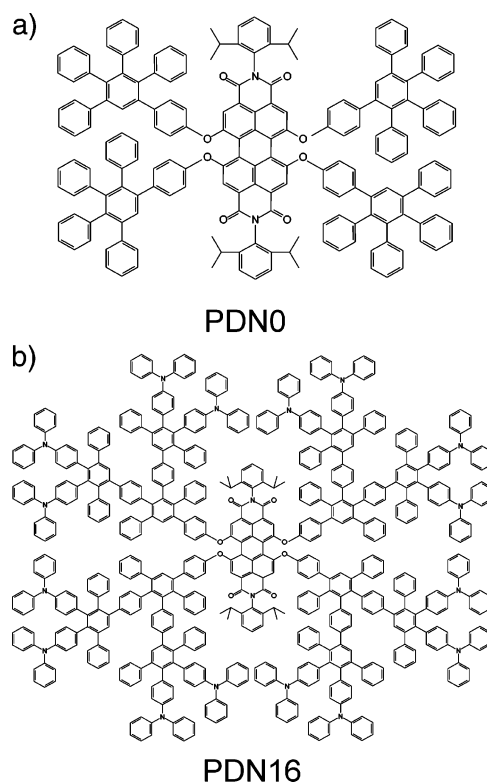


FIGURE 10. Structures of the perylene diimide derivatives studied by single-molecule spectroscopy: (a) PDN0 is the model compound; (b) PDN16 is the donor–acceptor system with 16 triphenylamine groups.

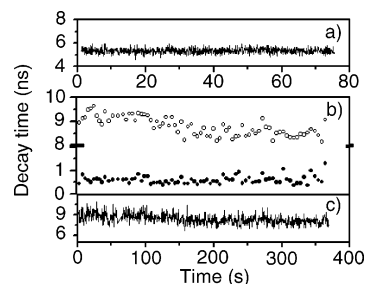
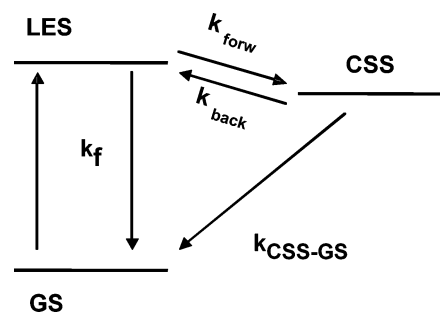


FIGURE 11. PDN16 in Zeonex (a) binned at 500 photons per decay and analyzed as a single exponential, (b) decay time of PDN16 in panel a binned at 10 000 photons per decay and analyzed with biexponential fit, and (c) the long time component of the decay in PS binned at 500 photons per decay.

Scheme 2. Forward ET from LES to CSS and Reverse ET from CSS to LES for PDN16 in Polystyrene (PS)



model. The trace shows no lifetime fluctuations during the measurement (Figure 12a). In contrast, when a single PDN16 molecule, which undergoes reversible ET, is

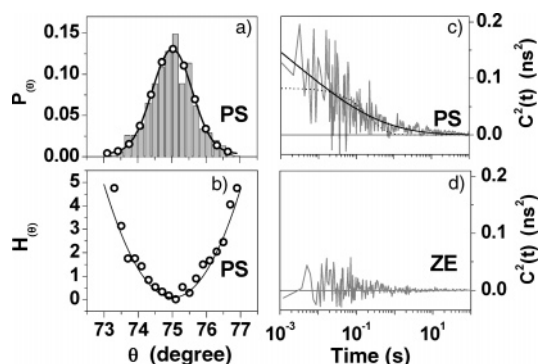


FIGURE 12. Panel a shows the distribution of through-bond donor–acceptor electronic coupling coordinate θ calculated on the basis of Figure 11c. Panel b shows the potential of mean force calculated from data in panel a (open circles). Also shown is a fit according to a harmonic model (line). Panel c shows autocorrelation of fluorescence decay time fluctuation calculated on a photon-by-photon basis for a single PDN16 molecule in PS (gray color). Also shown are single (dashed black line) and stretched (full black line) exponential fits. Panel d shows autocorrelation of fluorescence decay time fluctuation calculated on a photon-by-photon basis for a single PDN16 molecule in Zeonex.

probed in PS, fluctuations are seen in both forward and reverse ET related decay times (Figure 11b).²⁴ Here, single-molecule decay times were estimated from bins of 10 000 photons by MLE fitting with a biexponential model accounting for forward and reverse ET to determine accurately both short and long decay times.¹²

Fluctuations are even clearer to see in the backward ET related decay times (Figure 11c). They are much broader than the expected standard deviation from MLE and than the lifetime fluctuation of single PN16 molecules in ZE (Figure 12c). What is the origin of these decay time fluctuations detected in PS? The rate constant for non-adiabatic ET can be described as $k_{\text{ET}} = (4\pi^2/h)H^2\text{FCWD}$. Here h is the Planck's constant, H is the electronic coupling between the LES and the CSS, and $\text{FCWD} = (4\pi\lambda k_{\text{B}}T)^{-1/2} \exp[-(\Delta G^\circ + \lambda)^2/(4\lambda k_{\text{B}}T)]$ is the Franck–Condon weighted density of states with λ being the reorganization energy and ΔG° the free enthalpy. Fluctuations in lifetime or rate constant can arise from changes in FCWD or in H , that is, from fluctuations in the free enthalpy or D–A distance/orientation coupling. Assuming a three-state model, the forward and reverse ET rate constants from the related decay times and their contributions can be calculated, and the rate constants show a strong positive correlation suggesting that the fluctuations originate from changes in the electronic coupling H . From these values, we estimate a variation in the free energy of charge separation from -300 to $+200$ cal/mol. Thus, for this particular example, the LES and the CSS are energetically almost equal. If originating from changes in ΔG° , the fluctuations in decay time and hence rate constant for forward and reverse ET should anticorrelate with each other, while experimentally they correlate.²⁴

In view of the distance between donor and acceptor,²⁴ ET is governed in PDN16 by a through-bond mechanism and, hence, changes in the delocalization of the electronic density in the HOMO of the donor. Next to the donor,

adjacent phenyl rings from the dendritic branch are twisted with a dihedral angle of about 75° . Small changes in the dihedral angle, as small as few degrees, can lead to rather large changes in the delocalization of the donor HOMO over the polyphenylene branch. If the extent of the delocalization varies, the through-bond D–A electronic coupling will also vary. Consequently, fluctuations in decay times originate from small fluctuations of the dihedral angle of the adjacent phenyl rings next to the donor, a torsional motion known as libration.²⁵ In this assumption, the electronic coupling H follows an angular dependence of the form $H = H_0 \cos(\theta)$, θ being the torsion angle between adjacent phenyl rings next to the donor, and so does the rate constant for ET, $k_{\text{ET}}(\theta) = k_{\text{ET}_0} \cos^2(\theta)$.²⁵ Changes in the electronic coupling lead to correlated fluctuations of the rate constants for forward and reverse ET. This is an important aspect since it allows extraction of information about the fluctuations in the D–A coupling coordinate θ by following only the rate constant of reverse ET. From the probability density of the reverse ET related decay times and assuming an average torsional angle $\theta_{\text{avg}} = 75^\circ$, we next compute the probability density of θ , $P(\theta)$ (Figure 12a). $P(\theta)$ can be used to build the potential of the mean force according to $H(\theta) = -k_{\text{B}}T \ln[P(\theta)]$ (Figure 12b). Fitting $H(\theta)$ with a harmonic model, that is, $H(\theta) = k_{\text{B}}T(\theta - \theta_{\text{avg}})^2/(2\alpha_\theta)$, results in a variance $\alpha_\theta = 0.63 \text{ deg}^2$, a value larger than the error introduced by the MLE analysis (here 0.18 deg^2) and that reflects changes in θ as large as 4° (Figure 12b).

Although indicative of through-bond D–A coupling fluctuations, $H(\theta)$ provides only a static picture with no information on the time scale on which fluctuations occur. Dynamic information can be obtained by monitoring the reverse ET related decay time. Using bins of 500 photons, we can access lifetime fluctuations as fast as hundreds of milliseconds. Eventual dynamic changes occurring in a time scale shorter than the bin are missed. Therefore we applied a recently developed photon-by-photon analysis,²⁶ which can retrieve dynamic changes with high temporal resolution (up to the inverse of the detected photon count rate) and over a broad time range, from submillisecond to tens of seconds.

For a single dye molecule not showing lifetime fluctuations, $C^2(t) = 0$.²⁶ For a single molecule probing multiple conformations, $C^2(t)$ becomes multiexponential, reflecting the time range of k^{-1} fluctuations. $C^2(0)$ gives the variance of k^{-1} . In the assumption that for a single molecule the fluorescence intensity and the lifetime are correlated, $C^2(t)$ can be constructed on a photon-by-photon basis. Shown in Figure 12d is the $C^2(t)$ from a single PDN16 molecule in Zeonex. As expected, when no ET is present, the lifetime shows no correlation, that is, $C^2(t) = 0$. Figure 12c is the $C^2(t)$ of the single PDN16 molecule in PS accounting for the data shown in Figure 12b. Here, $C^2(t)$ was constructed only with delayed photons related to reverse ET. The decay of $C^2(t)$ spans several decades, from tens of milliseconds, where it shows the highest amplitude, up to seconds. A single-exponential decay model cannot characterize the decay of $C^2(t)$, and hence, we used a stretch exponential,

$M(t) = M(0) \exp(-(t/\tau_0)^\gamma)$ with $\tau_0 = 1.1$ ms and $\gamma = 0.17$, which reflects a distribution of lifetimes covering a broad time range (Figure 12c).

Libration of adjacent phenyl rings, the process responsible for the changes in through-bond D–A coupling, is a vibrational motion known to occur in solution in the picosecond time range.²⁷ Immobilization of PDN16 in a polymer matrix definitely slows such a motion, up to milliseconds. However, the fluctuations that we observe span a broad time range, from milliseconds to seconds (Figure 12c). Polymer motion will induce fluctuations in the decay time in the seconds time scale through changes in the local polarity of the donor involved in ET or eventually lead to switching between donor moieties within the same molecule seen here as a change in ΔG° and hence in the FCWD.

Conclusions and Perspectives

This Account clearly shows that single-molecule spectroscopy of well-chosen systems allows an investigation of fundamental photophysical processes, energy- or electron-transfer-based, occurring in these systems in much greater detail. It also shows that, on the other hand, knowledge of the ensemble photophysics is a must to fully understand the single-molecule behavior. Single-molecule spectroscopy allowed better understanding of the three FRET-based processes and visualization of one process, singlet–triplet annihilation, not observed in ensemble spectroscopy. It allowed estimation of the contribution of a novel pathway from a higher excited-state opened by singlet–singlet annihilation and demonstration of the role of a small local energy difference in trapping the excitation energy upon hopping between chromophores. In directional energy transfer, the Gaussian distribution of rates of energy transfer draw a better picture of the origin of the spread in transfer rate constants than the analysis of the ensemble data. As for electron transfer, the observation of the fluctuation of the rate constant of electron transfer with time for one molecule and the explanation based on torsional motion and mobility of the embedding polymer chains cannot be envisioned by ensemble measurements.

The fundamental processes observed and analyzed in these multichromophoric systems will of course also play a role in other synthetic, such as conjugated polymers, or biomolecular, such as Dsred, multichromophoric systems if the right conditions for energy or electron transfer are present.

Where here the focus was on the processes of the systems studied, having a detailed understanding of these systems, one can turn around the approach and use the observed phenomena playing on a length scale of several tens of nanometers (energy transfer) all the way to the angstrom scale (electron transfer) to investigate the role and importance of the “local environment” on the different parameters and hence try to get an idea on a very small length scale of the distribution of values related to different properties of the surrounding matrix.

Support from FWO, the Flemish Ministry of Education (Grant GOA 2/01), the BMBF, and the Federal Science Policy of Belgium (Grant IUAP-V-03) is acknowledged. A Max Planck Research Award to F.D.S. is also acknowledged. We also thank the many collaborators as well from Leuven and from Mainz that played a part in the development of the above-described results. Special thanks also to our partners M. Sauer (coincidence spectroscopy), J. Enderlein (wide-field microscopy), and S. Xie (photon-by-photon analysis).

References

- (1) (a) De Schryver, F. C.; Bhardwaj, I.; Put, J. Intramolecular photocycloaddition of *N,N'*-alkylbismaleimides. *Angew. Chem.* **1969**, *8*, 213–214. (b) De Schryver, F. C.; Boens, N.; Huybrechts, J.; Daemen J.; De Brackeleire M. Photochemistry of bichromophoric compounds: Scope and expectations. *Pure Appl. Chem.* **1977**, *49*, 237–247.
- (2) (a) De Schryver, F. C.; Collart, P.; Vandendriessche, J.; Goedeweck, R.; Swinnen A. M.; Van der Auweraer, M. Intramolecular excimer formation in bichromophoric molecules linked by a short flexible chain. *Acc. Chem. Res.* **1987** *20*, 159–166. (b) Van der Auweraer, M.; De Schryver, F. C.; Verbeek, G.; Vaes, A.; Helsen, N.; Van Haver, P.; Depaemelaere, S.; Terrell, D.; De Meutter S. Photoinduced electron transfer in polychromophoric systems. *Pure Appl. Chem.* **1993**, *65*, 1665–1670.
- (3) (a) VandenBout, D. A.; Yip, W. T.; Hu, D. H.; Fu, D. K.; Swager, T. M.; Barbara, P. F. Discrete Intensity Jumps and Intramolecular Electronic Energy Transfer in the Spectroscopy of Single Conjugated Polymer Molecules. *Science* **1997**, *277*, 1074–1077. (b) Huser, T.; Yan, M.; Rothberg, L. J. Single chain spectroscopy of conformational dependence of conjugated polymer photophysics. *Proc. Natl. Acad. Sci. U.S.A.* **2000**, *97*, 11187–11191.
- (4) (a) Bopp, M. A.; Jia, Y. W.; Li, L. Q.; Cogdell, R. J.; Hochstrasser, R. M. Fluorescence and photobleaching dynamics of single light-harvesting complexes. *Proc. Natl. Acad. Sci. U.S.A.* **1997**, *94*, 10630–10635. (b) Bopp, M. A.; Sytnik, A.; Howard, T. D.; Cogdell, R. J.; Hochstrasser, R. M. The dynamics of structural deformations of immobilized single light-harvesting complexes. *Proc. Natl. Acad. Sci. U.S.A.* **1999**, *96*, 11271–11276. (c) Cotlet, M.; Hofkens, J.; Habuchi, S.; Dirix, G.; Van Guyse, M.; Michiels, J.; Vanderleyden, J.; De Schryver, F. C. Identification of different emitting species in the red fluorescent protein DsRed by means of ensemble and single molecule spectroscopy. *Proc. Natl. Acad. Sci. U.S.A.* **2001**, *98*, 14398–14403.
- (5) (a) Morgenroth, F.; Reuther, E.; Müllen, K. Polyphenylene dendrimers: From three-dimensional to two-dimensional structures. *Angew. Chem., Int. Ed. Engl.* **1997**, *36*, 631–634. (b) Morgenroth, F.; Berresheim, A. J.; Wagner, M.; Müllen, K. Spherical polyphenylene dendrimers via Diels–Alder reactions: the first example of an A(4)B building block in dendrimer chemistry *Chem. Commun.* **1998**, *10*, 1139–1140. (c) Rosenfeldt, S.; Dingenouts, N.; Potschke, D.; Ballauff, M.; Berresheim, J.; Müllen, K.; Lindner, P. Analysis of the spatial dimensions of fully aromatic dendrimers. *Angew. Chem., Int. Ed.* **2004**, *43*, 109–112.
- (6) (a) Seybold, G.; Wagenblast, G. New perylene and violanthrone dyestuffs for fluorescent collectors. *Dyes Pigm.* **1989**, *11*, 303–317. (b) Holtrup, F. O.; Müller, G. R. J.; Quante, H.; De Feyter, S.; De Schryver, F. C.; Müllen, K. Terrylenimides: New NIR fluorescent dyes. *Chem.–Eur. J.* **1997**, *3*, 219–225.
- (7) Förster, T. Intermolecular energy migration and fluorescence *Ann. Phys.* **1948**, *2*, 55–75. Translated by R. S. Knox, Department of Physics and Astronomy, University of Rochester, Rochester, NY 14627.
- (8) Maus, M.; De, R.; Lor, M.; Weil, T.; Mitra, S.; Wiesler, U. M.; Herrmann, A.; Hofkens, J.; Vosch, T.; Müllen, K.; De Schryver, F. C. Intramolecular Energy Hopping and Energy Trapping in Polyphenylene Dendrimers with Multiple Peryleneimide Donor Chromophores and a Terryleneimide Acceptor Trap Chromophore. *J. Am. Chem. Soc.* **2001**, *123*, 7668–7676.
- (9) (a) Jordens, S.; De Belder, G.; Lor, M.; Schweitzer, G.; Van der Auweraer, M.; Weil, T.; Herrmann, A.; Wiesler, U. M.; Müllen, K.; De Schryver, F. C. Energy transfer within perylene-terrylene dendrimers evidenced by polychromatic transient absorption measurements. *Photochem. Photobiol. Sci.* **2003**, *2*, 177–186. (b) De Belder, G.; Schweitzer, G.; Jordens, S.; Lor, M.; Mitra, S.; Hofkens, J.; De Feyter, S.; Van der Auweraer, M.; Herrmann, A.; Weil, T.; Müllen, K.; De Schryver, F. C. Singlet–Singlet annihilation in multichromophoric Peryleneimide dendrimers determined by Fluorescence Upconversion. *ChemPhysChem* **2001**, *2*, 49–55.

- (10) Vosch, T.; Cotlet, M.; Hofkens, J.; Van Der Biest, K.; Lor, M.; Weston, K.; Tinnefeld, P.; Sauer, M.; Latterini, L.; Müllen, K.; De Schryver, F. C. Probing Förster type energy pathways in a first generation rigid dendrimer bearing two perylene imide chromophores. *J. Phys. Chem. A* **2003**, *107*, 6920–6931.
- (11) Hofkens, J.; Maus, M.; Gensch, T.; Vosch, T.; Cotlet, M.; Köhn, F.; Herrmann, A.; Müllen, K.; De Schryver, F. C. Probing photophysical processes in individual multichromophoric dendrimers by single molecule spectroscopy. *J. Am. Chem. Soc.* **2000**, *122*, 9278–9288.
- (12) (a) Hofkens, J.; Schroeyers, W.; Loos, D.; Cotlet, M.; Köhn, F.; Vosch, T.; Maus, M.; Herrmann, A.; Müllen, K.; Gensch, T.; De Schryver, F. C. Triplet states as nonradiative traps in multichromophoric entities: Single molecule spectroscopy of an artificial and natural antenna system. *Spectrochim. Acta, Part A* **2001**, *57*, 2093–2107. (b) Hofkens, J.; Cotlet, M.; Vosch, T.; Tinnefeld, P.; Weston, K. D.; Ego, C.; Grimsdale, A.; Müllen, K.; Beljonne, D.; Brédas, J.-L.; Jordens, S.; Schweitzer, G.; Sauer, M.; De Schryver, F. C. Revealing competitive Förster-type resonant energy transfer pathways in single bichromophoric molecules. *Proc. Natl. Acad. Sci. U.S.A.* **2003**, *100*, 13146–13151.
- (13) Hofkens, J.; Vosch, T.; Cotlet, M.; Habuchi, S.; Van Der Biest, K.; Müllen, K.; Dirix, G.; Michiels, J.; Vanderleyden, J.; Sauer, M.; De Schryver, F. C. Excited-state processes in individual multichromophoric systems. *Proc. SPIE—Int. Soc. Opt. Eng.* **2003**, *4962*, 1–10.
- (14) Böhmer, M.; Enderlein, J. Orientation imaging of single molecules by wide-field epifluorescence microscopy. *J. Opt. Soc. Am. B* **2003**, *20*, 554–559.
- (15) Schroeyers, W.; Vallée, R.; Digambra, P.; Hofkens, J.; Habuchi, S.; Vosch, T.; Cotlet, M.; Müllen, K.; Enderlein, J.; De Schryver, F. C. Fluorescence lifetimes and emission patterns probe the 3D-orientation of the emitting chromophore in a multichromophoric system. *J. Am. Chem. Soc.* **2004**, *126*, 14310–14311.
- (16) (a) Lounis, B.; Moerner, W. E. Single photons on demand from a single molecule at room temperature. *Nature* **2000**, *407*, 491–493. (b) Tinnefeld, P.; Weston, K. D.; Vosch, T.; Cotlet, M.; Weil, T.; Hofkens, J.; Müllen, K.; De Schryver, F. C.; Sauer, M. Antibunching in the emission of a single tetrachromophoric dendritic system. *J. Am. Chem. Soc.* **2002**, *124*, 14310–14311.
- (17) Tinnefeld, P.; Müller, C.; Sauer, M. Time-varying photon probability distribution of individual molecules at room temperature. *Chem. Phys. Lett.* **2001**, *345*, 252–258.
- (18) Tinnefeld, P.; Hofkens, J.; Herten, D.-P.; Masuo, S.; Vosch, T.; Cotlet, M.; Habuchi, S.; Müllen, K.; De Schryver, F. C.; Sauer, M. Higher excited-state photophysical pathways in multichromophoric systems revealed by single-molecule fluorescence spectroscopy. *ChemPhysChem* **2004**, *5*, 1786–1790.
- (19) Masuo, S.; Vosch, T.; Cotlet, M.; Tinnefeld, P.; Habuchi, S.; Bell, T. D. M.; Oesterling, I.; Beljonne, D.; Champagne, B.; Müllen, K.; Sauer, M.; Hofkens, J.; De Schryver, F. C. Multichromophoric dendrimers as single-photon sources: a single-molecule study. *J. Phys. Chem. B* **2004**, *108*, 16686–16696.
- (20) Schweitzer, G.; Gronheid, R.; Jordens, S.; Lor, M.; De Belder, G.; Weil, T.; Reuther, E.; Müllen, K.; De Schryver, F. C. Intramolecular directional energy transfer processes in dendrimers containing perylene and terylene chromophores. *J. Phys. Chem. A* **2003**, *107*, 3199–3207.
- (21) Cotlet, M.; Gronheid, R.; Habuchi, S.; Stefan, A.; Barbafina, A.; Müllen, K.; Hofkens, J.; De Schryver, F. C. Intramolecular directional Förster resonance energy transfer at the single molecule level in a dendritic system. *J. Am. Chem. Soc.* **2003**, *125*, 13609–13617.
- (22) (a) Lu, H. P.; Xie, X. S. Single-molecule kinetics of interfacial electron transfer. *J. Phys. Chem. B* **1997**, *101*, 2753–2757. (b) Knemeyer, J. P.; Marme, N.; Sauer, M. Probes for detection of specific DNA sequences at the single-molecule level. *Anal. Chem.* **2000**, *72*, 3717–3724. (c) Zang, L.; Liu, R.; Holman, M. W.; Nguyen, K. T.; Adams, D. M. A single-molecule probe based on intramolecular electron transfer. *J. Am. Chem. Soc.* **2002**, *124*, 10640–10641. (d) Yang, H.; Luo, G.; Karnchanaphanurach, P.; Louie, T.; Rech, I.; Cova, S.; Xun, L.; Xie, X. S. Protein conformational dynamics probed by single-molecule electron transfer. *Science* **2003**, *302*, 262–266.
- (23) Lor, M.; Thielemans, J.; Viaene, L.; Cotlet, M.; Hofkens, J.; Weil, T.; Hampel, C.; Müllen, K.; Verhoeven, J. W.; Van der Auweraer, M.; De Schryver, F. C. Photoinduced electron transfer in a rigid first generation triphenylamine core dendrimer substituted with a peryleneimide acceptor. *J. Am. Chem. Soc.* **2002**, *124*, 9918–9925.
- (24) Gronheid, R.; Stefan, A.; Cotlet, M.; Hofkens, J.; Qu, J.; Müllen, K.; Van der Auweraer, M.; Verhoeven, J. W.; De Schryver, F. C. Reversible intramolecular Electron Transfer at the Single Molecule Level. *Angew. Chem.* **2003**, *42*, 4209–4214. Cotlet, M.; Masuo, S.; Luo, G.; Hofkens, J.; Van der Auweraer, M.; Verhoeven, J.; Müllen, K.; Xie, X. S.; De Schryver, F. C. Probing conformational dynamics in single donor–acceptor synthetic molecules via photoinduced reversible electron transfer. *Proc. Natl. Acad. Sci. U.S.A.* **2004**, *101*, 14343–14348.
- (25) Davis, W. B.; Ratner, M. A.; Wasielewski, M. R. Conformational gating of long distance electron transfer through wire-like bridges in donor-bridge-acceptor molecules. *J. Am. Chem. Soc.* **2001**, *123*, 7877–7886.
- (26) Yang, H.; Xie, X. S. Probing single-molecule dynamics photon by photon. *J. Chem. Phys.* **2002**, *117*, 10965–10979.
- (27) Neto, N.; Muniz-Miranda, M.; Angeloni, L.; Castalucchi, E. Normal-mode analysis of 2,2'-bipyridine-I. Internal modes. *Spectrochim. Acta* **1983**, *39*, 97–106.

AR040126R